

Trace multi-class organic explosives analysis in complex matrices enabled using LEGO®-inspired clickable 3D-printed solid phase extraction block arrays

Rachel C. Irlam^a Cian Hughes^b Mark C. Parkin^c Matthew S. Beardah^d
Michael O'Donnell^d Dermot Brabazon^b Leon P. Barron^{ae}

^aDepartment Analytical, Environmental & Forensic Sciences, King's College London, 150 Stamford St., London SE1 9NH, United Kingdom

^bAdvanced Processing Technology Research Centre, Dublin City University, Dublin 9, Ireland

^cEurofins Forensic Services, Teddington, Middlesex, United Kingdom

^dForensic Explosives Laboratory, Dstl, Fort Halstead, Sevenoaks, Kent, United Kingdom

^eEnvironmental Research Group, Imperial College London, 80 Wood Lane, London W12 0BZ, United Kingdom

Corresponding author. E-mail address: leon.barron@imperial.ac.uk

Abstract

The development of a new, lower cost method for trace explosives recovery from complex samples is presented using miniaturised, click-together and leak-free 3D-printed solid phase extraction (SPE) blocks. For the first time, a large selection of ten commercially available 3D printing materials were comprehensively evaluated for practical, flexible and multiplexed SPE using stereolithography (SLA), PolyJet and fused deposition modelling (FDM) technologies. Miniaturised single-piece, connectable and leak-free block housings inspired by Lego® were 3D-printed in a methacrylate-based resin, which was found to be most stable under different aqueous/organic solvent and pH conditions, using a cost-effective benchtop SLA printer. Using a tapered SPE bed format, frit-free packing of multiple different commercially available sorbent particles was also possible. Coupled SPE blocks were then shown to offer efficient analyte enrichment and a potentially new approach to improve the stability of recovered analytes in the field when stored on the sorbent, rather than in wet swabs. Performance was measured using liquid chromatography-high resolution mass spectrometry and was better, or similar, to commercially available coupled SPE cartridges, with respect to recovery, precision, matrix effects, linearity and range, for a selection of 13 peroxides, nitramines, nitrate esters and nitroaromatics. Mean % recoveries from dried blood, oil residue and soil matrices were $79 \pm 24\%$, $71 \pm 16\%$ and $76 \pm 24\%$, respectively. Excellent detection limits between 60 fg for 3,5-dinitroaniline to 154 pg for nitroglycerin were also achieved across all matrices. To our knowledge, this represents the first application of 3D printing to SPE of so many organic compounds in complex samples. Its introduction into this forensic method offered a low-cost, 'on-demand' solution for selective extraction of explosives, enhanced flexibility for multiplexing/design alteration and potential application at-scene.

Keywords: 3D printing, Solid phase extraction, Forensic science, Complex matrices
High resolution mass spectrometry

To cite this article: Rachel C. Irlam, Cian Hughes, Mark C. Parkin, Matthew S. Beardah, Michael O'Donnell, Dermot Brabazon, Leon P. Barron, Trace multi-class organic explosives analysis in complex matrices enabled using LEGO®-inspired clickable 3D-printed solid phase extraction block arrays, / Journal of Chromatography A 1629 (2020) 461506.

1. Introduction

Forensic analysis of pre- and post-blast explosives residues is an ever-evolving challenge. Unfortunately, the frequency of criminal and terrorist activities involving explosives is increasing. The threats posed by improvised and commercially available explosive materials and their precursors require flexible and adaptable strategies for their detection, often at very low quantities and in different matrices of varying complexity. Forensic examination usually involves swabbing contaminated surfaces and/or transport of debris directly to the laboratory before analysis [1]. Many volatile explosives and marking agents sublime or transform easily in matrix and can be lost in storage or in transit [2], [3]. Therefore, some element of sample preparation at-scene may be an attractive option to improve stability, minimise matrix effects and improve throughput at the laboratory.

Solid phase extraction (SPE) is a well-established technique for explosives recovery [4], [5], [6], but there is still a need for more flexibility, sensitivity and selectivity for broad application to multi-class analysis in diverse sample types simultaneously submitted to a forensic laboratory. We recently evaluated SPE sorbent combinations for removal of matrix and extraction of 13 trace organic explosives from complex and forensically relevant sample types [7], [8]. In some cases, this improved detection limits by ~10-fold and enabled the trace detection of ng L^{-1} concentrations of 2,4,6-trinitrotoluene (TNT), 2,4-dinitrotoluene (2,4-DNT), 3,4-DNT and 1,3-dinitrobenzene (1,3-DNB) in urban wastewater from London. However, the use of two or more SPE cartridges was not cost-effective for large-scale monitoring and was cumbersome to multiplex. Miniaturised and multiplexed SPE platforms (e.g., 96-well SPE plates) arguably lack flexibility to easily integrate different/new sorbents and/or multiple, equally configurable layers of sorbent into extraction platforms and do not allow the user to alter the commercial housing design (e.g., to better manage fluid flow, to integrate additional connections or configure with instrumental analysis platforms). Online and/or micro-scale SPE approaches, such as microextraction in packed syringe (MEPS) [9], have been investigated for explosives and have also achieved ng L^{-1} LODs in aqueous samples [10], [11], [12], [13], [14]. Matrix effects, however, remain a similar problem, due to a limited number of suitable sorbents available and the inability to couple different sorbents together for enhanced selectivity. MEPS syringes are also prone to blocking, struggle to handle volumes larger than 500 μL and typically use sorbent masses of only 1-2 mg, which limit their suitability for high sensitivity forensic analysis. Therefore, better approaches that combine the advantages of several methodologies in a more flexible way are needed. This becomes especially important for at-scene pre-treatment, which may enhance the detection probability for unstable/volatile compounds [15], [16], [17], [18], [19] and enable safer and more practical transit of loaded cartridges instead of liquid samples. Additional advantages of field pre-treatment could also include increased throughput, sensitivity, quantitative accuracy and precision in the laboratory. The possibility for implementation of miniaturised, bespoke and on-demand devices that are tailorable to sample type could contribute to mitigating matrix effects, whilst also providing a feasible solution to on-site sample preparation, and, therefore, have significant advantages. One such technology that could represent an ideal means to fabricate such devices is 3D printing.

The emergence of 3D printing for rapid, inexpensive and convenient fabrication has led to its widespread use in a number of fields, including medicine, biology [20], [21], [22] and engineering/microfluidics [23], [24], [25], [26], [27], [28]. Examples of its use also for sample preparation and analytical purposes have emerged [29], [30], [31], [32], [33], [34], [35], [36], [37], [38], [39]. Regarding SPE in

particular, very few studies exist, especially for broad application using different chemical conditions. Su et al. recently removed unwanted salt matrix and achieved ng L^{-1} detection limits for trace elements in seawater using a 3D-printed polyacrylate-based preconcentrator [30]. Kataoka et al. 3D-printed a micro-SPE housing in polylactic acid (PLA) packed with Teflon and silica-based particles for pre-treatment of petroleum, with a 10-fold reduction in sample preparation time and recoveries >98% for the target maltene compounds [33]. De Middelée et al. developed a 3D-printed SPE scaffold, based on poly- ϵ -caprolactone with an integrated MIP, for a psychoactive drug, metergoline [40]. Kalsoom et al. used multi-material fused deposition modelling (MM-FDM) 3D printing to fabricate a housing for passive sampling based on PLA and acrylonitrile butadiene styrene, which performed similarly to the conventional alternative [41]. Previous works, however, have not exploited the potential to use dual-sorbent SPE to offer reduced matrix effects and higher sensitivity for organic explosives in complex samples [7]. The manufacture of modular blocks containing microfluidic channels [21], [42], [43], [44], [45], [46] with embedded sorbents could offer several advantages for miniaturised, more practical and field deployable SPE at much reduced cost. 3D printing multiple small, 'clickable' components at once could be time effective, result in little/no SPE cartridge stockpiling and eliminate delivery time for urgent forensic casework. Build designs could be shared electronically once a suitable material were found and shipment of liquid samples would not be needed if samples were extracted onto the sorbent in the field. Furthermore, bespoke threading or luer fitting designs could facilitate configuration with syringes, instrumentation or standard tubing. Ideally, the SPE housings should also be fritless, to enable easier integration of either commercially available sorbents or tailored functionalised chemical sorbents, such as MIPs, monoliths or hydrogels, as required by the user. Currently, however, few 3D printing materials have been shown to be compatible with both organic solvents and the extremes of pH and pressure typically observed in SPE or packed-bed microfluidics [34], [47], [48], [49]. For example, after testing nylon, polypropylene, acrylonitrile butadiene styrene, polyethylene terephthalate and polylactic acid (PLA), Kataoka et al. found that, for the application of 3D-printed parts to sample preparation of petroleum, PLA was the most suitable, displaying the least swelling in nonpolar and aromatic solvents, including n-heptane and toluene. Siporsky et al., however, reported the hydrolysis of PLA in acetonitrile, a common elution solvent in SPE [50], which represents a significant problem if it is to be applied. The potential for leaching of 3D-printed materials, as well as their physical stabilities in a variety of solvents, acids, bases and the potential for integration of sorbents typically used in SPE, requires further work before such materials can be reliably used routinely.

The aim of this work was, therefore, to develop robust and flexibly adaptable 3D-printed SPE blocks that could be clicked together for at-scene sample extraction of a range of different organic explosives and related compounds. Many of the selected analytes were volatile or prone to degradation and, therefore, sample-dependent on-site extraction could enhance the likelihood of their detection and provide increased assurance for forensic providers. A range of commercially available 3D printing materials and block designs were investigated with respect to (a) compatibility with SPE-relevant solvents/pH and analyte-3D-printed material interactions, (b) the performance of reproducibly printing a frit-free block design, (c) tolerance for flow rates typically observed in packed-bed SPE, (d) recovery of explosives, (e) matrix effect mitigation through multi-block, leak free arrays and (f) potential for trace quantitative analysis in complex samples using liquid chromatography-high resolution mass spectrometry (LC-HRMS). The stability of extracted explosives on-cartridge was also tested and compared

to that in liquid extracts. To our knowledge, this is the first 3D-printed solution for at-site SPE of multiple organic contaminants and the first for forensic explosives analysis. It is also the first to offer a comprehensive solution to matrix removal using tailored multi-sorbent SPE Lego®-style 'brick' arrays.

2. Experimental

2.1. Reagents and materials

HPLC or analytical grade acetonitrile, methanol, ethanol, isopropanol, dichloromethane, ethyl acetate, toluene and hexane were purchased from Fisher Scientific (Loughborough, UK). Ultrapure water was supplied by a Millipore Synergy-UV water purification system at 18.2 M Ω cm (Millipore, Bedford, USA). Ammonium acetate (>99% purity) and ammonium chloride (>99% purity) were sourced from Sigma-Aldrich (Gillingham, Dorset, UK), potassium hydroxide (85%) from BDH Laboratory Supplies (Poole, UK) and sulphuric acid (98%) from VWR Chemicals (Leicestershire, UK). Standard solutions at either (a) 1000 mg L⁻¹ (purity given in parenthesis for each) of each of 4-nitrotoluene (4-NT, 99.2%), 2,6-dinitrotoluene (2,6-DNT, 100.0%), 3,4-dinitrotoluene (3,4-DNT, 100%), TNT (100.0%), nitrobenzene (NB, 99.8%), 1,3,5-trinitrobenzene (TNB, 97.5%), nitroglycerin (NG, 99.4%), pentaerythritol tetranitrate (PETN, 99.4 %), erythritol tetranitrate (ETN, 99.9%), HMX (99.1%), RDX (98.6%) and 3,5-dinitroaniline (3,5-DNA, 100.0%); or (b) 100 mg L⁻¹ of each of hexamethylene triperoxide diamine (HMTD, 100.0%) and triacetone triperoxide (TATP, 99.1%) were prepared from stock reference materials sourced from Accustandard (New Haven, CT, USA). Ethylene glycol dinitrate (EGDN, 99.0%) at 1000 mg L⁻¹ was sourced from Thames Restek (Saunderton, Buckinghamshire, UK). 2,3-dimethyl-2,3-dinitrobutane (DMDNB, 98.0%) was obtained from Sigma Aldrich (Gillingham, Dorset, UK). Mixed working solutions at 50 or 5 mg L⁻¹, depending on the starting concentration and mode of analysis (LC-UV or LC-HRMS), were prepared in HPLC grade acetonitrile from each stock solution on the day of use and stored in the dark at -20°C.

2.2. 3D-printing and SPE block manufacturing procedures

Ten different materials were evaluated as potentially suitable for 3D-printed SPE housings. In the main, material safety datasheets described these as mainly acrylate/methacrylate blends along with a limited selection of other types. Materials included a (*PLA*)/*polyhydroxyalkanoic acid (PHA) blend* from ColorFabb, Belfeld, The Netherlands; *Nylon* (a nylon/caprolactam blend) from MarkForged, Cambridge, USA; *Clear Resin* and *Black Resin* (both methacrylate oligomer/monomer-based blends) from Formlabs, Berlin, Germany; *PlasCLEAR v2.0* (a methacrylate blend) from Puretone Ltd., Kent, UK; *VeroWhite*, *VeroBlack*, *RGD450* and *DURUS* (all acrylate blends) from Stratasys, Rheinmünster, Germany; and *Freeprint® Clear* (acrylate blend) from Detax GmbH, Ettlingen, Germany. A range of different 3D printers, depending on the material, were evaluated. These included an Ultimaker 2 for FDM in *PLA/PHA* (Ultimaker B.V., Utrecht, Netherlands); a MarkOne for FDM in *Nylon* (Markforged Inc.); a Form2 for SLA of all Formlabs resins (Formlabs); the Connex1 Objet260 (Stratasys) for PolyJet printing of *VeroWhite/Black*, *RGD450* and *DURUS*; and either an Asiga Freeform Pico Plus27 or Asiga MAX Mini 3D printer (Puretone Ltd.) for SLA of *PlasCLEAR v2.0*. These ten materials were chosen based on their compatibilities with the three main additive manufacturing techniques used in microfluidics (SLA, FDM and PolyJet printing). These printers were also the only 3D printing modes that were accessible at the time. Acrylate/methacrylate materials have been used in microfluidics for many years [51]. Limited work has been done so far concerning 3D printing sample preparation devices,

but *PLA/PHA* was specifically chosen for testing here based on work by Kataoka et al., who used PLA to fabricate sample preparation devices for extracting target compounds from complex petroleum samples [36]. *Nylon* was chosen for its potential stability in some SPE-related solvents and safety for user handling. Metal-based materials were not initially considered here due to the current associated cost and speciality required for printing of potentially large numbers of small consumable items for routine application in practicing forensic laboratories. For microscopy of printed parts, a VHX2000E 3D Digital Microscope (Keyence, Osaka, Japan) at x10 or x100 magnification fitted with a 54-megapixel 3CCD camera was used both to image and measure the dimensions of 3D-printed parts. For initial chemical stability experiments, 1 cm³ cubes (n=6) were printed in each material until PlasCLEAR v2.0 was eventually selected as the preferred material for prototype SPE housings. Computer-aided designs (CAD) were generated using SolidWorks 2016/17 or 2017/18 software (Dassault Systems, Waltham, MA, USA), converted to .STL format and uploaded to the SLA 3D printer using Asiga Composer software (Asiga, Anaheim Hills, CA, USA). Ultimately, an SLA printer was chosen, since the most suitable resin from initial material testing, PlasCLEAR, was SLA-compatible. Therefore, the SPE component was designed based on this mode of 3D printing. Optimised parts were oriented vertically on the build platform, with the inlet face-down, since horizontal channels were found to be prone to blockage as a result of ‘back-side effect’, as reported also by Gong et al. [52]. The print time was approximately 1.5 h for up to nine blocks simultaneously and the cost per block was ~GBP 0.65p. Full build parameters (Table S1) and .STL files for the finalised designs are detailed in the supplementary information. After printing, the parts were rinsed with IPA and any uncured resin removed *via* vacuum suction using a vacuum aspirator (Bel-Art™ SP Scienceware, NJ, USA). Finally, based on previous methods used by O’Neill and Gong, the parts were immersed in IPA, sonicated for 10 min (Branson 5510 40 kHz sonicator) and left to dry in air [24], [53], [54].

The sorbents from three commercially available SPE cartridges were depacked, including Isolute ENV+ (Biotage, Uppsala, Sweden), Strata Alumina-N (Phenomenex, Cheshire, UK) and HyperSep SAX (Thermo Fisher Scientific). Coupled blocks were used for matrix removal and analyte concentration, as needed. No frits were required. With respect to packing of matrix removal blocks, one of two options were chosen depending on the matrix: (a) 20 mg of Strata Alumina-N was used in a single block for oil and blood matrices or (b) 10 mg of Strata Alumina-N to pack the SPE outlet followed by 10 mg HyperSep SAX (for soil) layered on top. These two matrix removal sorbents (Strata Alumina-N and HyperSep SAX) were chosen based on previous work in our lab, which showed little/no sorption of the target analytes [17]. Serial combination with analyte-selective cartridges for each of the different matrices tested herein were also based on that work (optimised). For analyte concentration blocks, 10 mg of Isolute ENV+ were added for all matrices. For the packing, the relevant mass of dry sorbent was weighed onto a piece of folded paper using an analytical balance and transferred into the block.

2.3. Instrumentation

The exact composition of PlasCLEAR v2.0 resin was proprietary and therefore qualitative analysis using ¹H, ¹³C, ³¹P, ¹H-correlation spectroscopy (¹H-COSY), heteronuclear multiple bond correlation (HMBC) and heteronuclear multiple-quantum correlation (HMQC) nuclear magnetic resonance (NMR) spectroscopy was conducted on the resin using a 400 MHz Avance III Bruker NMR spectrometer (Bruker UK Limited, Coventry, UK), carried out in deuterated chloroform at standard temperature and pressure.

For leak and pressure assessments of the 3D-printed SPE blocks, a Prominence HPLC System (Shimadzu, Milton Keynes, UK) was used to pump ethanol:water (50:50 % v/v) through blocks at flow rates of 0.1-10 mL min⁻¹. For initial recovery assessments, conditioning solvent and sample were delivered to the SPE device at 1 mL min⁻¹ and the elution solvent at 0.5 mL min⁻¹ automatically *via* a Gynkotec M300 CS HPLC pump (Gynkotec, Germering, Germany) and then thereafter manually at ~1-2 mL min⁻¹, maintained using a timer, *via* a 10 mL polypropylene syringe (Sigma Aldrich, Gillingham, UK) for method performance assessment in matrix. The backpressure generated by the 3D-printed SPE cartridges was enough to enable a constant flow rate through the configured blocks and acceptable precision was obtained.

For measurements of the solvent stability, leaching and analyte sorption properties of the 3D-printed SPE blocks, as well as explosives analysis involving liquid chromatography coupled to ultraviolet detection (LC-UV), an Agilent 1100 series LC instrument (Agilent Technologies, Cheshire, UK) was used at detection wavelengths of 210 and 254 nm. Separations were performed on a 10 × 2.1 mm ACE C₁₈-AR guard column coupled to a 150 × 2.1 mm, 3.0 μm ACE C₁₈-AR analytical column (Hichrom Ltd, Reading, UK). The mobile phase flow rate was 0.15 mL min⁻¹, the column oven was 20°C and the injection volume was 5 μL. Gradient elution was performed using 8 mM ammonium acetate in water:methanol 90:10 (v/v) (mobile phase A) and 8 mM ammonium acetate in water:methanol 10:90 (v/v) (mobile phase B) over 40 min. Initial mobile phase composition was 40 % B, which was then raised to 100 % B over 30 min and then held for 10 min before returning to 40 % B and equilibrating for 34.5 min (total run time = 75 min). For LC-HRMS analysis, an Accela HPLC coupled to an Exactive™ instrument (Thermo Fisher Scientific, San Jose, CA, USA) was used, as described previously [7]. Briefly, the same C₁₈-AR column, injection volume and oven temperature were used for all separations. Gradient elution at 0.3 mL min⁻¹ using 0.2 mM ammonium chloride in water:methanol 90:10 (v/v) (mobile phase C, apparent pH 7.5) and 0.2 mM ammonium chloride in water:methanol 10:90 (v/v) (mobile phase D, apparent pH 7.5) was performed over 39 min according to the following programme: 40 % D at 0 min; linear ramp to 95 % D over 15 min; to 100 % D over 0.50 min; hold at 100 % D for 5.5 min; return to 40 % D over 0.50 min; re-equilibration for 17.5 min. Samples were kept at 10°C throughout the analysis. The heated atmospheric pressure chemical ionisation source (APCI) was operated in either positive (m/z 50-400) or negative modes (m/z 60-625) using full-scan high resolution at 50,000 FWHM in separate runs. Data was processed using Thermo Xcalibur v 2.0 software.

2.4. Sample types and preparation procedures

Characterised topsoil was purchased from Springbridge Direct Ltd. (Uxbridge, UK) and stored at 4°C in Nalgene bottles until analysis. The soil had the following properties: pH (100 g L⁻¹) was 5.5-6.0; particle size distribution of 0-12 mm; and a density of 200-250 g L⁻¹, and, as compost, was primarily made up of organic material. For extraction into 10 mL EtOH:H₂O (50:50 % v/v), 3 g of standardised topsoil were weighed and transferred into an Ultra-Turrax® ball mill extraction cartridge with a glass bead (IKA, Oxford, UK) and spun for 10 min at 3200 rpm (optimised). This device is small (100 × 40 × 160 mm), portable and battery operable, enabling its use in the field, as required. After 30 min settling, and prior to SPE with 3D-printed blocks, ~5 mL of supernatant were diluted to 10 mL with ultrapure water for SPE. For SPE using commercial cartridges, 5 g of soil were first extracted as above and ~10 mL of the supernatant were diluted to 20 mL before SPE. Fortification with explosives was performed by spiking soil directly with a standard prepared in acetonitrile at 2.5 μg g⁻¹ after the weighing step. Soil was then air dried before extraction. For application of the method to contaminated soil, samples were provided by the Forensic Explosives Laboratory (FEL, UK) from six different locations that are regularly used for munitions and explosives activities. Duplicate

samples were taken from each site and extracted as above, before undergoing 3D-printed SPE and LC-HRMS screening.

Pooled whole human blood from five volunteers (500 μL) was pipetted onto glass microscope slides (Thermo Fisher, Paisley, UK) and dried on a hotplate at 40°C. Oil residues were taken from a range of household kitchens that primarily used olive and sunflower oil for open-pan cooking. For sampling, cotton wool swabs were purchased from Sainsbury's (London, UK). For swabbing at scene, the standard operating procedure used by the UK Forensic Explosives Laboratory was employed. Briefly, cotton wool was wetted with EtOH:H₂O (50:50 %v/v) and was lightly wiped across the contaminated surface with forceps, using both sides of the swab once. It was then returned to a glass vial containing 5 mL EtOH:H₂O (50:50 %v/v), then agitated and compressed thoroughly within the solvent using a glass Pasteur pipette (~1 min/side). This vial was then sealed with a septum lined cap for transport and/or storage until analysis. At the laboratory, the solvent was then drawn up through the swab with a pipette and transferred into a 20 mL volumetric flask. For SPE using commercially available cartridges, another 5 mL EtOH:H₂O (50:50 %v/v) were added to the swab and the agitation and transfer process repeated. The resulting extract (~10 mL) was diluted to 20 mL in a volumetric flask with water and transferred to a clean, dry Nalgene bottle. For SPE using 3D-printed components, 5 mL water were added to the swab and the agitation and transfer process repeated. The resultant extract was diluted to 10 mL with water.

2.5. Solid phase extraction

Multi-cartridge SPE of all extracts was performed using commercially available cartridges or 3D-printed/packed SPE blocks. For commercial cartridges, dual-cartridge SPE was performed using previously optimised procedures and sorbents were selected based on the matrix [7]. For blood and oil, Alumina-N (500 mg x 3 mL barrel) and Isolute ENV+ (100 mg x 6 mL barrel) were coupled. Both cartridges were conditioned with 1 mL 50:50 EtOH:H₂O. For soil, Hypersep SAX (200 mg x 3 mL barrel) was coupled to Isolute ENV+ (100 mg x 6 mL barrel) and conditioned with 1 mL of 0.1% formic acid in EtOH:H₂O (50:50 %v/v). A volume of 20 mL of all samples was loaded onto the dual-cartridge set-up without pH adjustment, as it had little effect on the recovery of explosives [8]. Extraction was performed under vacuum using a 12-port SPE manifold (Phenomenex, Torrance, CA) at pressures ≤ 20 kPa. After loading, the matrix removal sorbent was discarded and the second cartridge eluted in 1 mL acetonitrile, to give a concentration factor of 20.

In the finalised method employing 3D-printed SPE blocks for extraction of complex samples, a single matrix removal block and one analyte concentration block were required for dried blood and soil. However, an additional analyte concentration block was required for oil residues (i.e., three in total). Blocks were 'clicked' together directly and conditioned in the same way as commercial cartridges. For sample loading, 10 mL volumes were loaded at 1-2 mL min⁻¹ using positive pressure with a 10 mL syringe. The backpressure of ≤ 100 psi enabled consistent delivery by hand. Following this, the matrix removal block was removed and the remaining cartridge(s) eluted in 0.5 mL acetonitrile (again, to achieve a comparable concentration factor of 20 to that of the method using commercial SPE cartridges).

3. Results and discussion

3.1. 3D printing of click-together SPE blocks

Properties and characteristics of 3D-printed materials. One of the main purposes of this multi-sorbent, coupled SPE block approach was to minimise matrix effects. However,

unwanted interferents from manufacture, or leachables arising from exposure to different chemical conditions (e.g., solvents and pH), could result in ion suppression or enhancement in HRMS. Following immersion of 1 cm³ 3D-printed cubes of each material in vials of EtOH:H₂O (50:50 % v/v) under agitation for 1 h, the degree of leaching was examined using HPLC-UV. This solvent was chosen as it is used as the extraction solvent for swabs in the procedure currently employed at the Forensic Explosives Laboratory. As can be seen in Fig. 1(a), leaching occurred from most materials. Among the worst were Nylon, Formlabs Clear, Freeprint Clear and DURUS, with interferences eluting across the runtime at high intensities. Relatively interference-free chromatograms were obtained for PLA/PHA and PlasCLEAR and these were retained for further testing. It is important to note, however, that the print quality was clearly poorer for PLA/PHA cubes printed using FDM in comparison to PlasCLEAR by SLA. Furthermore, and upon exposure to n=7 additional polar/non-polar solvents over 1 h (Table S2), clear physical differences between these materials were observed. PLA/PHA degraded extensively and almost instantaneously when immersed in acetonitrile (the optimised elution solvent in this SPE procedure), making it unsuitable for this application. For most other solvents tested, distortions, splitting and discolouration of PLA/PHA was evident, particularly in dichloromethane, toluene and hexane. In alcohols, PLA/PHA remained visibly intact. PlasCLEAR, on the contrary, was far more stable in most organic solvents, with the exception of dichloromethane. In acetonitrile, it displayed excellent physical integrity, even for an extended period of up to 8 hours (albeit with some increased leaching evident, Fig. S1). As elution takes <1 min, the concentration of interfering leachables in acetonitrile extracts after SPE with PlasCLEAR blocks is likely to be much lower. Immersion of the PlasCLEAR parts in acetonitrile for 5 min did indeed show negligible leaching, as shown in the LC-HRMS chromatograms in Fig. S1b, indicating promising potential for use in SPE for trace explosives analysis. The exposure of cubes to 3 M H₂SO₄ and 1.2 M KOH for 1 hour also showed excellent physical stability, demonstrating potential flexibility for use in other SPE applications. As a result, PlasCLEAR was chosen as the best material to 3D print SPE blocks.

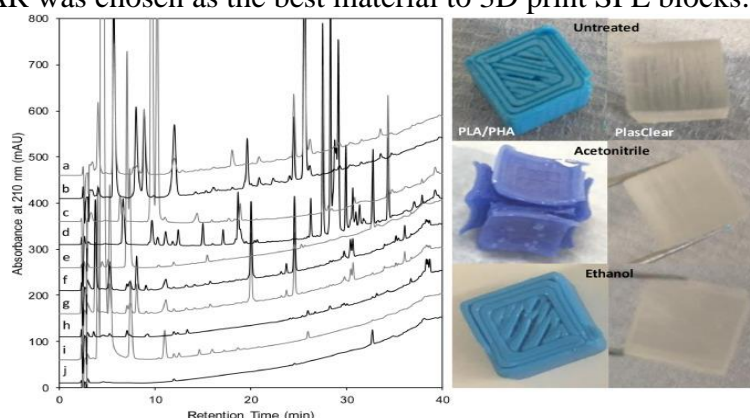


Fig. 1. Left: Overlaid LC-UV chromatograms of leachate from ten different 1 cm³ 3D-printed blocks following treatment in 50:50 EtOH:H₂O. Key: a – RGD450; b – DURUS; c – Formlabs Clear; d – Freeprint Clear; e – Formlabs Black; f – Verowhite; g – Veroblack; h – PlasCLEAR; I – Nylon; j – PLA/PHA. Right: Example PLA/PHA and PlasCLEAR blocks before treatment followed by agitation in MeCN and EtOH for 1 h.

In the first instance, the intended use of the 3D-printed component was as an SPE housing rather than as a sorbent material itself. Therefore, any sorption of the target compounds to the

material itself was undesirable as it could result in lower recoveries. Consequently, sorption to both PlasCLEAR and PLA/PHA was studied using LC-UV and a selection of explosives as probe species of differing hydrophobicity (predicted logP by ACDLabs from Chemspider, Royal Society of Chemistry, UK), including two nitramines (HMX, logP = -2.91; RDX, logP = -2.19), three nitroaromatics (TNB, logP = 1.22; TNT, logP = 1.68; and NB, logP = 1.95), an alkylnitrate (DMDNB, logP = 1.82) and a nitrate ester (NG, logP = 2.32). Mean sorption to PlasCLEAR was $3.7 \pm 3.4\%$ (n=21) following exposure at 2.5, 10 and 25 $\mu\text{g mL}^{-1}$ of all explosives in 50:50 EtOH:H₂O for 1 h. The only outlier was TNB with $7.4 \pm 5.8\%$ sorption across the three concentrations (Fig. S3). Despite its disintegration in acetonitrile, sorption to PLA/PHA for a subset of three explosives (NG, RDX and TNT) in EtOH:H₂O was also similarly low at $3.5 \pm 2.7\%$ across all three concentrations (Fig. S4), again highlighting its potential for application in other SPE methods.

NMR confirmed the presence of diurethane dimethacrylate (DUDMA) as the principal monomer in PlasCLEAR (Fig. S5). From ³¹P NMR in particular, Irgacure® 819 was established as the photo-initiator, since it is the only commercially available phosphorus-containing photo-initiator compatible with the wavelengths of 385 and 405 nm on the Asiga 3D printers used. The material safety datasheet for PlasCLEAR indicated tetrahydrofurfuryl methacrylate (THFMA) as a potential secondary monomer component present at a lower concentration, but neither this, nor the presence of any other ingredients, could be confirmed by NMR. Therefore, this preliminary study successfully identified a suitable 3D printing resin that could potentially be broadly applied across several SPE applications for the first time. It not only displayed good stability, low leaching and low sorption when subjected to different solvent chemistries, but, given its composition, the potential to chemically bond a sorbent to PlasCLEAR components could also be investigated. In this first phase of work, however, it was decided to pack the 3D-printed SPE blocks with commercially available sorbents, in order to compare their performance with standard barrel SPE cartridges for the recovery of trace explosives and allow easy and more accessible adoption by end-user labs in the short term.

Design of fritless 3D-printed SPE blocks. Despite discovery of a suitable material, the design of SPE blocks presented additional challenges. A difficulty encountered in microfluidic and miniaturised devices for preparation/analytical purposes is the design and integration of frits, weirs or other physical features to trap sorbents [55]. To negate a frit entirely, the principle of the particulate keystone effect was implemented [56], [57]. Previous work has shown that particles formed a barrier at outlets approximately three-fold wider than their own diameter [57]. Here, the sorbent bed was tapered from a diameter of 4.90 mm to 400 μm in the design software, as the lowest printable dimension that was repeatably clearable post-build (Fig. 2). Following 3D printing of n=112 blocks, the actual outlet diameter was found to be $543 \pm 14 \mu\text{m}$ (example microscope image shown in Fig. S2). The difficulty with successfully printing channels narrower than 500 μm in diameter is a result of the so-called ‘overcuring effect’, experienced also by other groups [54], [58]. This diameter was sufficiently large to allow the complete removal of uncured resin post-build, whilst also allowing solution to pass through unhindered. The achieved diameter was also narrow enough to hold most sorbent particle types in place without losses. HyperSep SAX particle sizes (40-60 μm), however, were too small to effectively block the SPE block outlet. Strata Alumina-N was slightly larger on average (i.e., 120 μm). Therefore, where required, Hypersep SAX was layered on top of Strata Alumina-N to overcome this problem and, if needed, this combination of both could be applied for matrix removal more generally. A fritless solution to sample preparation brings several benefits, primarily that it was more practical, simple and less time-consuming to manufacture.

It was also particularly advantageous for trace analysis, by eliminating problems that can be caused by frits, including potential analyte sorption, clogging by matrix and additional manufacturing-based interference that could be introduced from frit components. These potential issues stemming from the frit have been acknowledged by a number of manufacturers and depend largely on the application.

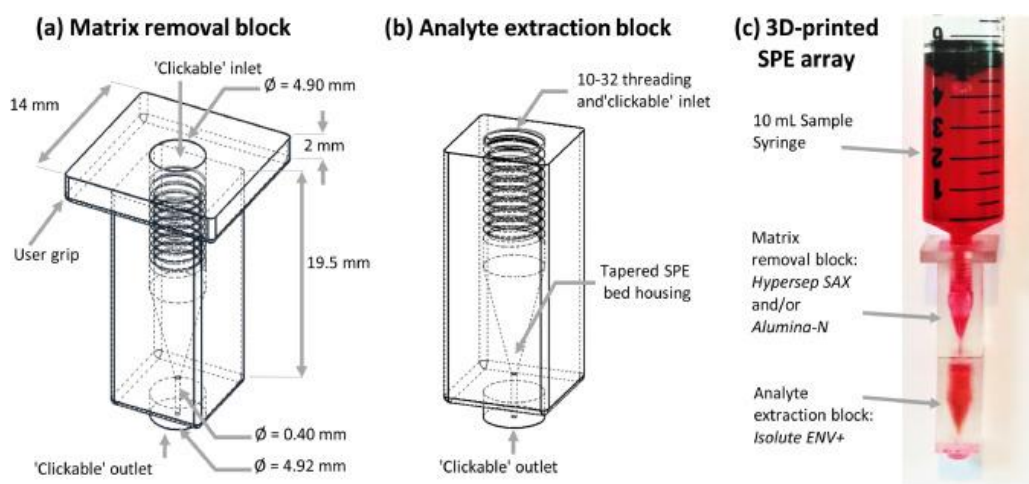


Fig. 2. 3D-printed SPE block housing manufactured in PlasCLEAR for the extraction of explosives residues from complex matrices including (a) the matrix removal block design, and (b) analyte extraction blocks. In (c) the complete 3D-printed SPE array is shown with two connected blocks in series and configured directly to a 10 mL syringe with a solution of red dye to show the leak-free flow path design. Components with both Luer and 10-32 threaded fittings could be configured directly to all inlets.

The last requirement of this 3D-printed design was to allow direct coupling with other SPE blocks and LC instrumentation if needed (e.g. for online SPE applications) [59]. Threaded inlets complementary with standard 10-32 fittings enabled configuration to an HPLC pump to deliver solvent to packed blocks at flow rates of up to 10 mL min^{-1} ($n=16$). No leaking was observed at the thread fitting or anywhere else across the block. In a Lego®-inspired design, the outlet and inlet dimensions of two sorbent-packed blocks were optimised to also enable them to 'click' together, resulting in leak-free delivery of solvent across both blocks, which has not, to our knowledge, been demonstrated before for SPE. Threading of the outlet to match threading of the inlet was also tested, but print quality was found to be poor in some cases and the fit and seal not as good as when the surface was smooth. To make the connection process easier for the user and to aid with visual differentiation, the matrix removal cartridges incorporated a slightly larger square plate on the top. Backpressures were linear with flow rate for both single and coupled blocks containing all sorbents, with no leakage, excessive swelling or tolerance exceedance, and all had very similar flow rate vs. pressure slopes. For SPE loading, the optimised flow rate was $\sim 2 \text{ mL min}^{-1}$, which generated a backpressure of 4-5 bar, regardless of whether these were single or coupled SPE blocks (Fig. S6). Finally, the weights of all $n=112$ blocks above displayed a relative standard deviation of $<1\%$, which demonstrated excellent reproducibility, especially for a relatively low-cost SLA printer. After treatment with solvents, the block outlets (as the smallest dimension) were remeasured to assess swelling and no change was observed.

For all printing work described here, an Asiga SLA-based 3D printer was used, since the chosen PlasCLEAR material is SLA-compatible. It is worth noting, however, that a PolyJet printer was also tested (albeit not with PlasCLEAR and for simple comparison), but the narrow channel in the design was found to be unclearable, with support material still present after >24 h immersion in water to try to dissolve it.

3.2. SPE method development using 3D-printed blocks

Model solutions of 14 selected explosives at $5 \mu\text{g mL}^{-1}$ in EtOH:H₂O (25:75 %v/v) were used to optimise sample (2, 6, 10 and 20 mL, n=3) and acetonitrile elution volumes (100 μL -1000 μL , 100 μL increments, n=3). Peroxides were not included in this initial optimisation experiment as they lack a UV chromophore. During method development, a pump was used to control flow rates delivered to SPE cartridges, for added consistency. Recovery throughout this work was determined using the peak area ratio of analyte in the SPE extract and analyte in a matrix-matched standard at theoretical 100% recovery concentration. Using the same SPE procedure as for commercial dual-sorbent SPE cartridges (one for matrix removal, the other for analyte concentration), lower recoveries were achieved on 3D-printed blocks, likely due to lower sorbent mass. Modification of the method to a 10 mL sample volume and a 0.5 mL elution volume yielded an acceptable mean recovery of $62 \pm 19\%$ across all tested analytes. As expected, recoveries were lowest for polar compounds, such as HMX and RDX, likely due to self-elution. The elution profile in acetonitrile (Fig. S7) showed that all analytes were eluted from 3D-printed blocks in ~ 1 mL (77% mean recovery), but, as a compromise, it was decided to reduce the elution volume to 0.5 mL to improve sensitivity overall and to maintain a 20-fold concentration factor. The majority of analytes were also eluted to a high extent in this volume. The reusability of the blocks was also tested. Three used blocks were left to dry, the sorbent emptied (by simple inversion) and the blocks sonicated in IPA for 30 min. After drying in air, they were repacked with 10 mg SPE sorbent (Isolute ENV+), conditioned and 10 mL ethanol:water (25:75 % v/v) were passed through them *via* a syringe. No analyte-containing solution was loaded in this case, to check for carryover from the previous extraction. Following elution with 0.5 mL acetonitrile no carryover occurred, demonstrating the blocks could be successfully washed and reused. Whilst not likely to be exploited in forensic applications, this potential for reuse could be an attractive advantage in other fields, such as environmental analysis. Other types of organic compound were not investigated here, but the approach shows great promise for other forensically relevant small molecules or emerging contaminants, for example inorganic explosives, illicit drugs, pharmaceuticals and pesticides.

3.3. 3D-printed SPE and LC-HRMS of trace explosives in complex matrices

Matrix effects. The performance of the 3D-printed SPE procedure in a dual cartridge format was evaluated using cooking oil residue, soil and dried, whole human blood (Fig. 3). Matrix effects were generally <15 % across all sample types, which was excellent given their degree of complexity. It also demonstrated low matrix binding. For extracts of soil and swabs of cooking oil residues, no significant difference overall was found between the mean matrix effects after SPE using the 3D-printed approach and those obtained after the dual-sorbent approach with commercially available cartridges ($p > 0.05$), indicating that this new approach could be broadly applied to other compounds. However, for particular analytes such as TNB, NG and ETN, significant enhancement was observed in both of these matrices using 3D-printed SPE blocks. For cooking oil residue, variability across triplicate measurements was lower with the 3D-printed blocks overall. Low matrix effects were again observed in extracts of dried blood but, with 3D-printed components, suppression was more pronounced for 3,5-DNA, PETN and RDX, along with signal enhancement of TNB, as observed with oil residue and soil.

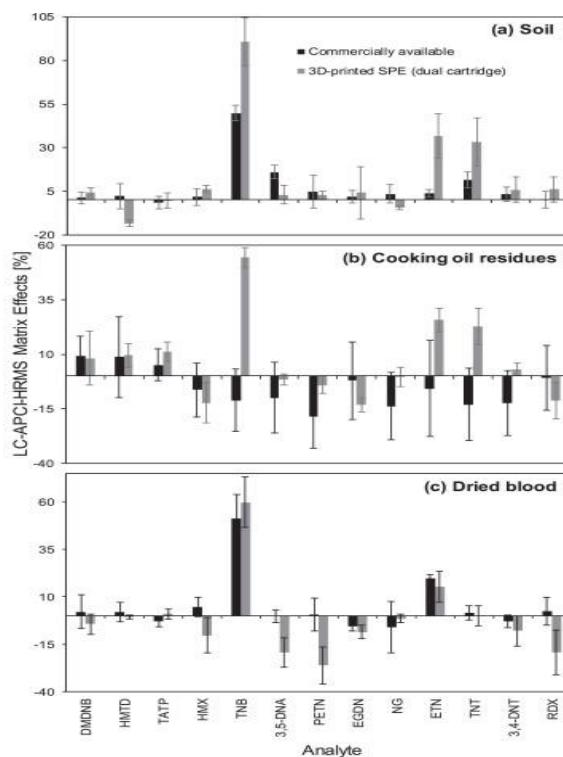


Fig. 3. Comparison of matrix effects on 13 selected explosives observed in (a) extracted soil, (b) extracted swabs of cooking oil and (c) extracted swabs of dried blood for both coupled 3D-printed SPE blocks and commercially available cartridges. The sample loading solvent was EtOH:H₂O (25:75 v/v).

Recovery and precision. The recoveries from dried blood swabs were excellent (Fig. 4), with an average recovery of 79% for the 13 tested analytes with no further amendments to the procedure required. The recoveries for explosives in soil and cooking oil residues, on the other hand, were initially found to be lower after using the 3D-printed assemblies. This was likely due to the 10-fold reduction in sorbent mass for analyte concentration, without an accompanied reduction in sample extracted (i.e., cooking oil residue on a swab or mass of soil). For soil, a breakthrough investigation using 0.5-5 g sample masses revealed masses above 3 g yielded markedly decreased recovery overall (Fig. S8). Therefore, a lower mass of 3 g was selected in comparison to commercial cartridges (5 g), without any further amendments to the SPE protocol needed. As it is impossible to control the amount of oil residue collected on a swab from a real crime scene, recoveries were significantly improved using a three-block combination, comprising a single matrix removal block followed by two analyte extraction blocks and no other changes to the procedure needed. This necessity for a second selective extraction block with cooking oil residues, but not soil or blood, was likely due to the complexity of the matrix. Previous work using dual-sorbent SPE combinations for mitigating matrix effects in complex samples showed cooking oil was consistently the most complex of those tested [17]. The main interferences in cooking oil residue included organic and highly hydrophobic compounds, which would likely be retained on the Isolute ENV+ sorbent, but also potentially the cartridge housing. Competitive sorption of interfering components from the cooking oil residue matrix was, therefore, potentially higher than that in blood or soil samples, which caused saturation of the sorbent and thus required addition of a second block to improve analyte recoveries. Hence, the potential to assemble a specific array based on the combination that yields the highest recoveries for a particular sample type is clearly beneficial,

demonstrating the highly advantageous nature of such a flexible approach. Once all final amendments were implemented, mean recoveries improved for dried blood, oil residue and soil matrices to $79 \pm 24\%$, $71 \pm 16\%$ and $76 \pm 24\%$, respectively, and, for dried blood and oil residue, were comparable to those observed using conventional cartridges [7]. No connective tubing was needed and all extractions could be performed using a handheld syringe fitted directly to the 3D-printed block inlet. The backpressures generated across coupled cartridges were enough to enable satisfactory manual control of the sample and eluting solvent flow rates. In addition to coupling identical blocks together, this approach offers the user much more control of how much sorbent packing is required in each block for the specific application, to minimise waste if more tailoring is needed and in a simplified manner.

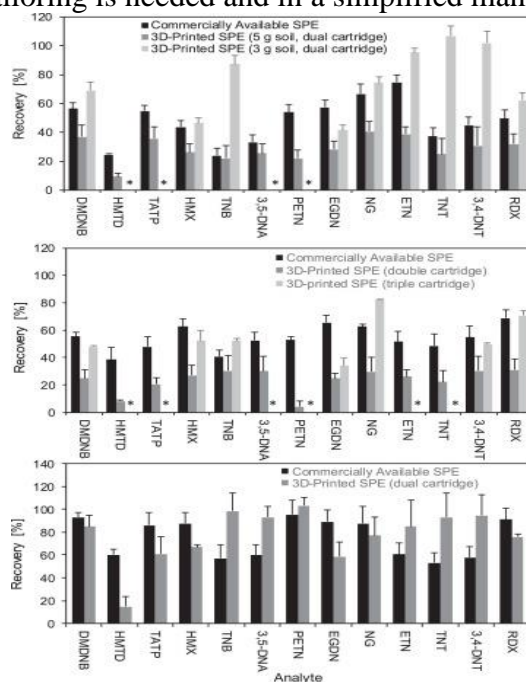


Fig. 4. Comparison of the recovery of 13 selected explosives using both sorbent-packed, 3D-printed, coupled SPE blocks and coupled commercially available cartridges for (a) extracted soil, (b) extracted swabs of cooking oil and (c) extracted swabs of dried blood. The sample loading solvent composition for SPE was 27:75 v/v EtOH:H₂O. For soil, extracted mass reduction from 5 g to 3 g is shown to demonstrate improved recovery. For cooking oil, the addition of a second analyte extraction 3D-printed block is shown for a selection of 7 explosives to demonstrate improved capacity (those marked with * were not included).

On-cartridge analyte stability. To test the ability for these SPE cartridges to be used in the field, the stability of dried, extracted residues on SPE blocks was examined over 10 days using LC-UV at room temperature ($\sim 25^\circ\text{C}$) for a selection of explosives (Fig. 6). To our knowledge, this work is the first to evaluate any added stability arising from storage on the SPE cartridge for explosives residues. The recovery and stability on the 3D-printed SPE cartridges here were compared to the standard protocol using swabs stored in 5 mL EtOH:H₂O (50:50 %v/v) and stored under the same conditions (analytes spiked at 5 mg L^{-1}). In general, good stability was observed for most analytes across this period using both approaches. Relative standard deviations of the peak area for all compounds on the 3D-printed SPE blocks were $<8\%$. Recovery for polar compounds HMX, RDX and DMDNB was lower, as expected, on SPE blocks, due to poorer sorbent interactions. On the other hand, recoveries for ETN and TNT were markedly higher and more stable on SPE blocks. In stored swabs, on the other hand, a

gradual loss of both compounds was observed (35% for ETN and 63% for TNT). Sisco et al. showed that out of six selected explosives, TNT and ETN transformed over relatively short periods of time under a variety of environmental conditions [60] and that their volatilities explained similar losses at 25 °C (vapour pressure ETN = 3.19×10^{-3} [61] and TNT = 9.15×10^{-9} [62]). Therefore, the 3D-printed SPE cartridges offered enhanced stability overall, combined with extra convenience, for ambient transport and storage over longer periods of time. Whilst sufficient repeats have been performed to confirm the reliability of the method, additional storage and transport conditions would be useful to study in greater detail but lay outside of the scope of the current work.

Other analytical performance characteristics. Excellent method performance (Table 1) was obtained across all three matrices and example extracted ion chromatograms in each matrix at low spiking concentrations are shown in Fig. 5. Measurements of linearity, range and limits of detection (LOD) were accrued according to International Council for Harmonisation of Technical Requirements for Pharmaceuticals for Human Use (ICH) method validation guidelines [63].

Table 1

Analytical performance characteristics according to ICH method validation guidelines for 3D-printed SPE and LC-HRMS of explosives in three different complex matrices and comparison to published methods. All SPE was performed using a hand-held syringe for sample and solvent delivery.

| Analyte | Quantitative Range ^a (pg on column) | | | Coefficient of Determination (R^2) ^b | | | Limit of Detection (LOD) ^c (this work, pg on column) | | | Previously Published LOD (pg on column) | | |
|---------|---|----------------------|-----------------------|---|-------------|-------------------|--|-------------|-------------|---|--------------------------|--------------------------|
| | Soil | Cooking Oil | Dried Blood | Soil | Cooking Oil | Dried Blood | Soil | Cooking Oil | Dried Blood | Soil | Cooking Oil ^e | Dried Blood ^e |
| | | | | | | | | | | | | |
| DMDNB | 41-1000 | 33-1000 | 10-1000 | 0.97 | 0.99 | 1.00 | 12.4 | 9.81 | 3.12 | 0.001 ^f | 21.2 | 33.8 |
| HMTD | 26-1000 | 27-500 | 72-500 | 0.99 | 0.99 | 0.98 | 7.83 | 8.17 | 21.7 | n.a. | 13.1 | 19.4 |
| TATP | 5-1000 | 20-500 | 12-500 | 0.96 | 0.99 | 0.97 | 1.60 | 6.01 | 3.71 | n.a. | 0.41 | 20.6 |
| HMX | 3-1000 | 39-500 | 0.4-500 | 0.99 | 0.99 | 1.00 | 0.97 | 11.73 | 0.11 | 0.1 ^f ; 8.0 ^g ; 23.9 ^h | 0.04 | 0.04 |
| TNB | 1-1000 | 1-500 | 0.3-500 | 0.99 | 0.99 | 0.99 | 0.32 | 0.21 | 0.09 | 1.82 ^h | 0.09 | 0.02 |
| 3,5-DNA | 0.2-1000 | 1-500 | 1-500 | 1.00 | 1.00 | 0.99 | 0.06 | 0.32 | 0.19 | 0.20 ⁱ | 0.03 | 0.07 |
| PETN | 113-1000 | 24-1000 ^d | 8-1000 | 0.98 | 0.99 | 1.00 | 34.0 | 7.11 | 2.38 | 0.01 ^f ; 3.16 ^h | 0.54 | 25.7 |
| NG | 513-2000 | 5-1000 ^d | 66-1000 | 0.99 | 1.00 | 0.99 | 153.9 | 1.63 | 19.9 | 0.001 ^f ; 4.43 ^h | 70.3 | 51.1 |
| ETN | 183-2000 | 122-1000 | 7-1000 | 0.98 | 0.98 | 0.99 | 55.0 | 36.5 | 2.20 | 0.001 ^f | 14.5 | 31.7 |
| TNT | 3-1000 | 3-500 | 1-500 | 0.99 | 1.00 | 0.98 | 0.97 | 0.77 | 0.17 | 0.001 ^f ; 3.0 ^h ; 1.53 ^h | 0.03 | 0.15 |
| 3,4-DNT | 2-1000 | 4-500 | 2-500 | 0.99 | 1.00 | 0.98 | 0.66 | 1.09 | 0.61 | 1.22 ^h | 0.13 | 0.12 |
| RDX | 2-1000 | 2-500 | 1-500 | 0.98 | 1.00 | 1.00 | 0.72 | 0.46 | 0.40 | 0.01 ^f ; 36.0 ^g ; 8.80 ^h ; 0.62 ⁱ | 0.01 | 0.03 |
| EGDN | 312-2000 | n.d. | 304-1000 ^d | 1.00 | n.d. | 0.96 ^d | 93.7 | 240 | 91.2 | 0.001 ^f ; 1.17 ^h | 48.8 | 55.0 |

n.d. Not determined

^a Lower value is the LOQ, determined using 10 x standard deviation of the peak area of n = 3 replicates of the lower range concentration tested divided by the slope of the calibration line in matrix. Higher value is the upper concentration tested in the range

^b Based on N_≥5 concentrations and processed by the optimised 3D-printed SPE, LC-HRMS method for each matrix unless otherwise indicated. Neat extracts were blank and background subtraction not required.

^c Determined using 3 x standard deviation of the peak area of n = 3 replicates of the lower range concentration limit divided by the slope of the calibration line in matrix

^d N=4 concentrations

^e Previous work in our laboratory using liquid extraction, dual sorbent commercially available SPE and the same LC-HRMS method [7]

^f Liquid extraction, SPE with gas chromatography-electron capture detection (GC-ECD) [4]

^g Ultrasonication, SPE and liquid chromatography-dielectric barrier discharge ionization-time of flight-mass spectrometry [73]

^h Liquid extraction and GC-MS [74]

ⁱ Liquid extraction and GC-ECD [75]

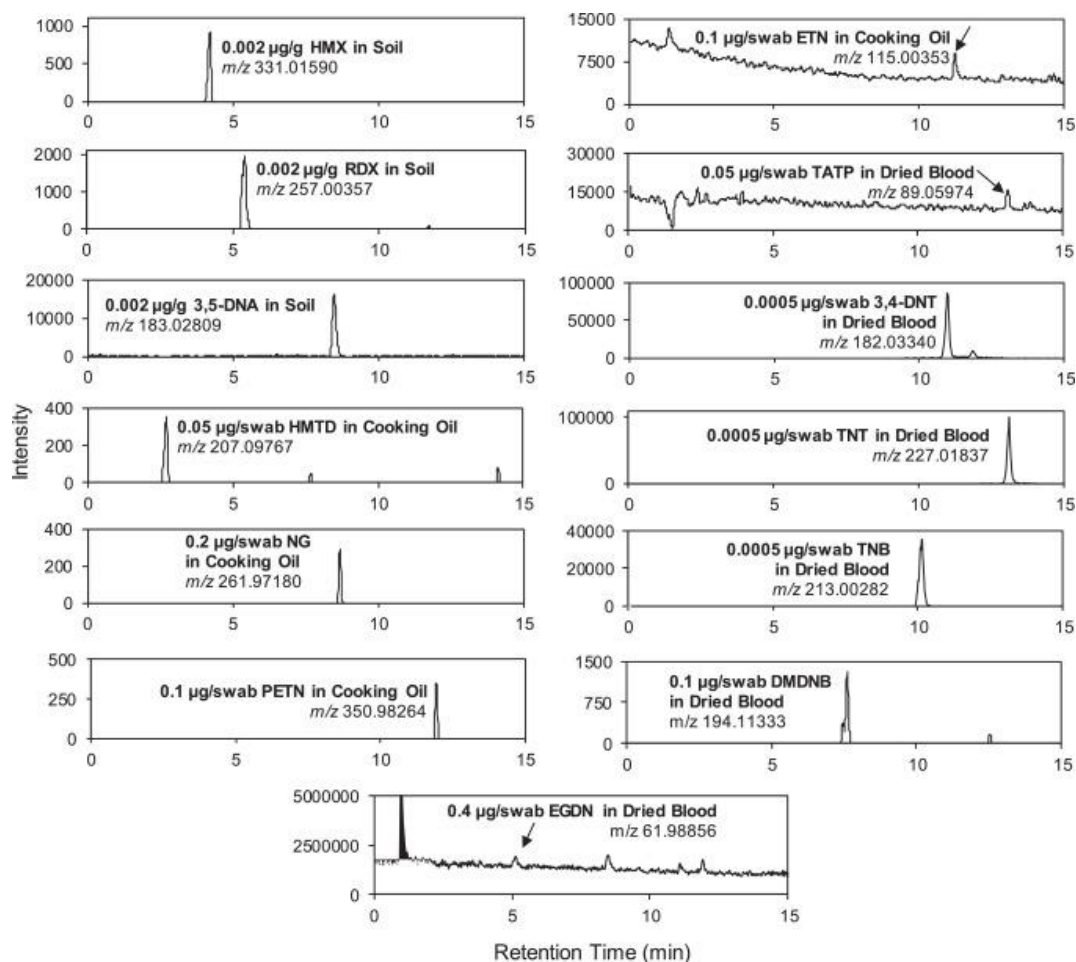


Fig. 5. A selection of extracted ion chromatograms of explosives residue in soil, cooking oil and dried blood matrices.

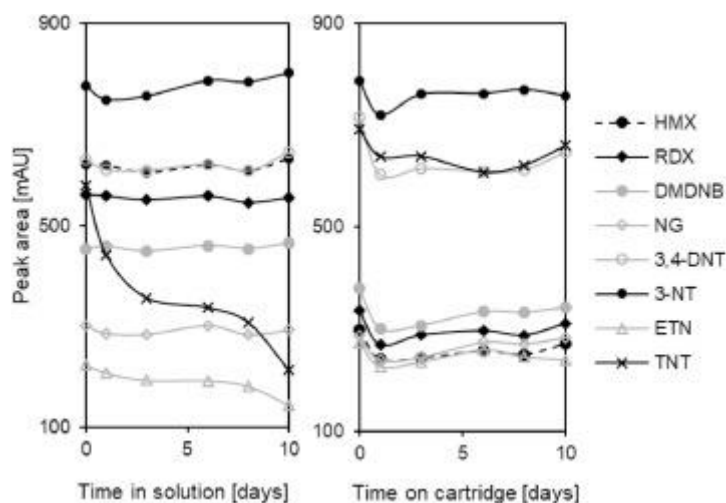


Fig. 6. Stability of selected explosives on (a) spiked swabs stored in EtOH:H₂O and (b) 3D-printed SPE blocks over 10 days at room temperature in model solutions following extraction. Analyte concentrations were 5 $\mu\text{g mL}^{-1}$. Swabs were stored in 5 mL MeCN over this period.

For most compounds, the method was linear over three orders of magnitude, with R^2 generally ≥ 0.99 , and LODs at the fg – pg on column range were achieved. Signal intensity for EGDN, however, was poor across the board and the method did not display sufficient analytical performance. The monitored m/z for EGDN corresponded to the nitrate anion and no other fragment was detectable, which made it unsuitable for confirmatory analysis. Recovery by 3D-printed SPE blocks was not the major cause, as shown in [Figs. 3](#) and [4](#). For all other compounds and across the three sample types, LODs were moderately higher in soils (~22 pg on average). That said, 3,5-DNA had the best LOD in soil across all sample types, tested at 60 fg. Sensitive, confirmatory methods using SPE and LC-MS for the quantitative determination of large numbers of explosives from soils are rare, especially for improvised explosives such as peroxides. LODs were, however, much poorer for PETN, NG and ETN and, for PETN and NG, only four calibrants could be used to assess linearity in cooking oil. Recovery was generally good in soil using 3D-printed SPE for these compounds. This was, therefore, attributed, instead, to lower HRMS sensitivity and this effect was observed across all three sample types tested. Two methods employing GC coupled to electron capture detection (ECD) were also selected for comparison. In particular, a method by Thomas et al. displayed excellent detection limits that were several orders of magnitude better in several different types of soil than this approach [\[4\]](#). This method employed liquid extraction into acetone and was followed by SPE. The added sensitivity that was observed here was likely due to ECD, as average recoveries from soil were relatively low ($48 \pm 7\%$). Therefore, the dual 3D-printed blocks could potentially add even more sensitivity to such a method, though the use of a confirmatory analytical detection technique, such as MS, is more desirable for forensic application.

For swabbed samples of contaminated cooking oil and dried blood, our previous work using the same analytical method but commercially available SPE pre-treatment was used as a direct comparator [\[7\]](#). Both approaches achieved LODs in the fg on-column level for the majority of compounds and were comparable or better than other works for some compounds ([Table 1](#)). For example, LODs were 6- to 14-fold better for PETN, ETN and TATP in particular using the 3D-printed blocks in blood. The latter two compounds are regularly used in improvised explosive devices in major terrorist incidents, including the 2015 Paris and 2007 London attacks. Furthermore, several peroxides like TATP have a high vapour pressure and sublime at room temperature. Therefore, sensitive methods are critical for this explosive type. The advantages of a rapidly assembled, sample specific and low-cost 3D-printed SPE array was therefore realised here, with the added benefit of potential at-scene use. Furthermore, this technology is also likely to benefit other field-based investigations, such as environmental monitoring and toxicology, for example.

3.4. Application to real soil samples

Application to contaminated soil samples from six different locations ([Table 2](#)) showed that several analytes could be detected with varying degrees of assurance (full information is given in [Tables S3](#) and [S4](#)). The retention times of all peaks deviated by $<2\%$ from the expected retention time and all accurate mass inaccuracies were <3 ppm, in line with standard procedures at FEL. The minimum criteria for identification at FEL include retention time and the primary ion and analyte occurrence is normally then confirmed using a second method. However, in the absence of a second, confirmatory technique here, additional ions for the majority of detected compounds were searched for to add assurance. The detection of only one ion could potentially, in many cases, be as a result of a low concentration, e.g., for DEDPU in Location 4. [Table S5](#) shows the extracted ion chromatograms of nine detected analytes in the soil. Tetryl,

though a legacy explosive compound, was not detected, but has been shown to transform rapidly in soil environments in <30 days [64], [65]. Walsh et al. extracted thousands of soil samples from sites potentially contaminated with explosives, including manufacturing plants, load and pack facilities and depots, and found that the major energetic-related compounds detected were TNT, RDX, TNB, 2,4-DNT, 1,3-DNB, 2-Am-4,6-DNT, 4-Am-2,6-DNT, HMX and tetryl [66], showing good agreement with the results presented here. The health hazards associated with TNT and RDX, such as carcinogenicity and mutagenicity, have made them, as well as their metabolites and related compounds, including the DNTs, Am-DNTs, DNBs, TNB and HMX, a priority for environmental monitoring programmes [67], [68], [69], [70], [71]. Consequently, it is crucial that they can be detected in matrix using current analytical methodologies, as successfully demonstrated here. This is the first time that a 3D-printed sample preparation technique has been implemented for the successful detection of trace concentrations of explosives compounds in soil. This harmonisation of analytical chemistry with 3D printing represents a pivotal point for flexible, multi-sorbent solid phase extraction approaches and could pave the way for further exploitation of additive manufacturing technology in the analytical arena.

Table 2
Analytes detected in soil across all six locations (colour key given below).

| Analytes detected | Location | | | | | |
|-------------------|----------|---|---|---|---|---|
| | 1 | 2 | 3 | 4 | 5 | 6 |
| DEDPU | | | | | | |
| RDX | | | | | | |
| HMX | | | | | | |
| 3,4-DNT | | | | | | |
| 2,6-DNT | | | | | | |
| 2,4-DNT | | | | | | |
| TNT | | | | | | |
| 4-Am-2,6-DNT | | | | | | |
| 2-Am-4,6-DNT | | | | | | |
| TNB | | | | | | |
| 1,3-DNB | | | | | | |

| Key |
|----------------------------|
| t_R + one ion detected |
| t_R + two ions detected |
| t_R + three ion detected |
| No ion detected |

4. Conclusion

Successful manufacture of field-deployable and miniaturised sample preparation devices for trace explosives residue recovery using a low-cost benchtop 3D printer was demonstrated and applied to multiple complex matrices for the first time. Using a diurethane dimethacrylate-based resin (PlasCLEAR), frit-free 3D-printed SPE blocks were packed with different

particulate sorbents and could be directly connected for both matrix removal and analyte concentration *via* a hand-held syringe. Recoveries of selected explosives using the 3D-printed devices were comparable to commercially available coupled SPE cartridges for soil, dried blood and cooking oil matrices but offered several additional advantages including: (a) greater flexibility to be packed with the amount and sorbent of choice by the user, (b) potential to multiplex and modify parts to generate tailored arrays for a particular sample type, with no additional tubing or connecting parts, (c) low-cost and easy accessibility for laboratories, (d) on-demand nature, enabling rapid production of parts, as required, with no ordering delay, (e) easy connection with syringes for on-site use, (f) good stability in a broad range of common organic solvents, which could allow application to extraction in other scientific fields, (g) ability to both preserve the sample and speed up the overall analytical process chain and (h) comparable performance with conventional SPE cartridges for the trace extraction of organic explosives. To our knowledge this approach is the first to show added stability of up to ten days for all analytes when extracted onto SPE blocks and particularly for selected volatile explosives, such as TNT and ETN, rather than storage on wetted swabs. Determination at the low-sub pg level in-matrix was possible for almost all analytes. Furthermore, a total of 11 organic explosives and related compounds were successfully detected in soils, demonstrating the applicability of the novel SPE approach in real situations. Ultimately, this approach offers new capability to forensic providers for on-demand, bespoke component manufacture to help increase throughput and reliability for complex sample analysis.

This work was approved by the BDM Research Ethics Subcommittee of King's College London (reference no. HR-17/18-4078) and has been kindly funded by the Environmental and Physical Sciences Research Council (Project Reference: 1812614) and Dstl (contract reference: DSTLX-1000106427). This research is supported in part by a research grant from Science Foundation Ireland (SFI) under Grant Number 16/RC/3872 and is co-funded under the European Regional Development Fund. Thanks are also extended to Claire Lock for her assistance with forensic explosives analysis training. The authors would also like to thank the Metropolitan Police Service (UK) for their invaluable advice and assistance with PLA/PHA 3D-printing. The authors declare no competing interests. LEGO® is a trademark of the LEGO Group of companies which does not sponsor, authorize or endorse this research.

References

[1] K. Szomborg, F. Jongekrijg, E. Gilchrist, T. Webb, D. Wood, L. Barron

Residues from low-order energetic materials: The comparative performance of a range of sampling approaches prior to analysis by ion chromatography

Forens. Sci. Int., 233 (2013), pp. 55-62

ArticleDownload PDFView Record in ScopusGoogle Scholar

[2] G.L. McEneff, B. Murphy, T. Webb, D. Wood, R. Irlam, J. Mills, D. Green, L.P. Barron

Sorbent film-coated passive samplers for explosives vapour detection part A: materials optimisation and integration with analytical technologies

Sci. Rep., 8 (2018)

Google Scholar

[3] G.L. McEneff, A. Richardson, T. Webb, D. Wood, B. Murphy, R. Irlam, J. Mills, D. Green, L.P. Barron

Sorbent film-coated passive samplers for explosives vapour detection part B: deployment in semi-operational environments and alternative applications

Sci. Rep., 8 (2018)

Google Scholar

[4] J.L. Thomas, C.C. Donnelly, E.W. Lloyd, R.F. Mothershead, M.L. Miller

Development and validation of a solid phase extraction sample cleanup procedure for the recovery of trace levels of nitro-organic explosives in soil

Forens. Sci. Int., 284 (2018), pp. 65-77

ArticleDownload PDFView Record in ScopusGoogle Scholar

[5] R. Tachon, V. Pichon, M.B. Le Borgne, J.J. Minet

Comparison of solid-phase extraction sorbents for sample clean-up in the analysis of organic explosives

J. Chrom. A, 1185 (2008), pp. 1-8

ArticleDownload PDFView Record in ScopusGoogle Scholar

[6] K. Levsen, P. Mussmann, E. Bergerpreiss, A. Preiss, D. Volmer, G. Wunsch

Analysis of nitroaromatics and nitramines in ammunition wastewater and in aqueous samples from former ammunition plants and other military sites

Acta Hydrochimica Et Hydrobiologica, 21 (1993), pp. 153-166

CrossRefView Record in ScopusGoogle Scholar

[7] R.C. Irlam, M.C. Parkin, D.P. Brabazon, M.S. Beardah, M. O'Donnell, L.P. Barron

Improved determination of femtogram-level organic explosives in multiple matrices using dual-sorbent solid phase extraction and liquid chromatography-high resolution accurate mass spectrometry

Talanta, 203 (2019), pp. 65-76

ArticleDownload PDFView Record in ScopusGoogle Scholar

[8] H. Rapp-Wright, G. McEneff, B. Murphy, S. Gamble, R. Morgan, M. Beardah, L. Barron

Suspect screening and quantification of trace organic explosives in wastewater using solid phase extraction and liquid chromatography-high resolution accurate mass spectrometry

J. Hazard. Mater., 329 (2017), pp. 11-21

ArticleDownload PDFView Record in ScopusGoogle Scholar

[9] G. Dhingra, P. Bansal, N. Dhingra, S. Rani, A.K. Malik

Development of a microextraction by packed sorbent with gas chromatography-mass spectrometry method for quantification of nitroexplosives in aqueous and fluidic biological samples

J. Separ. Sci., 41 (2018), pp. 639-647

CrossRefView Record in ScopusGoogle Scholar

[10] M. Smith, G.E. Collins, J. Wang

Microscale solid-phase extraction system for explosives

J. Chrom. A, 991 (2003), pp. 159-167

ArticleDownload PDFCrossRefView Record in ScopusGoogle Scholar

[11] R.L. Marple, W.R. LaCourse

A platform for on-site environmental analysis of explosives using high performance liquid chromatography with UV absorbance and photo-assisted electrochemical detection

Talanta, 66 (2005), pp. 581-590

ArticleDownload PDFView Record in ScopusGoogle Scholar

[12] S. Rodriguez-Mozaz, M.J.L. de Alda, D. Barcelo

Advantages and limitations of on-line solid phase extraction coupled to liquid chromatography-mass spectrometry technologies versus biosensors for monitoring of emerging contaminants in water

J. Chrom. A, 1152 (2007), pp. 97-115

ArticleDownload PDFView Record in ScopusGoogle Scholar

[13] H.R. Sobhi, H. Farahani, A. Kashtiaray, M.R. Farahani

Tandem use of solid-phase extraction and dispersive liquid-liquid microextraction for the determination of mononitrotoluenes in aquatic environment

J. Separ. Sci., 34 (2011), pp. 1035-1040

CrossRefView Record in ScopusGoogle Scholar

[14] Q.A. Sun, Z.L. Chen, D.X. Yuan, C.P. Yu, M. Mallavarapu, R. Naidu

On-line SPE coupled with LC-APCI-MS for the determination of trace explosives in water

Chromatographia, 73 (2011), pp. 631-637

CrossRefView Record in ScopusGoogle Scholar

[15] U. Ochsenbein, M. Zeh, J.D. Berset

Comparing solid phase extraction and direct injection for the analysis of ultra-trace levels of relevant explosives in lake water and tributaries using liquid chromatography-electrospray tandem mass spectrometry

Chemosphere, 72 (2008), pp. 974-980

ArticleDownload PDFView Record in ScopusGoogle Scholar

[16] S. Schramm, D. Leonco, C. Hubert, J.C. Tabet, M. Bridoux

Development and validation of an isotope dilution ultra-high performance liquid chromatography tandem mass spectrometry method for the reliable quantification of 1,3,5-Triamino-2,4,6-trinitrobenzene (TATB) and 14 other explosives and their degradation products in environmental water samples

Talanta, 143 (2015), pp. 271-278

ArticleDownload PDFView Record in ScopusGoogle Scholar

[17] R. Martel, A. Bellavance-Godin, R. Levesque, S. Cote

Determination of nitroglycerin and its degradation products by solid-phase extraction and LC-UV

Chromatographia, 71 (2010), pp. 285-289

CrossRefView Record in ScopusGoogle Scholar

[18] A. Halasz, C. Groom, E. Zhou, L. Paquet, C. Beaulieu, S. Deschamps, A. Corriveau, S. Thiboutot, G. Ampleman, C. Dubois, J. Hawari

Detection of explosives and their degradation products in soil environments

J. Chrom. A, 963 (2002), pp. 411-418

ArticleDownload PDFView Record in ScopusGoogle Scholar

[19] J. Pachman, R. Matyáš

Study of TATP: stability of TATP solutions

Forens. Sci. Int., 207 (2011), pp. 212-214

ArticleDownload PDFView Record in ScopusGoogle Scholar

[20] C. Chen, Y. Wang, S.Y. Lockwood, D.M. Spence

3D-printed fluidic devices enable quantitative evaluation of blood components in modified storage solutions for use in transfusion medicine

Analyst, 139 (2014), pp. 3219-3226

View Record in ScopusGoogle Scholar

[21] P.K. Yuen

SmartBuild-A truly plug-n-play modular microfluidic system

Lab on a Chip, 8 (2008), pp. 1374-1378

CrossRefView Record in ScopusGoogle Scholar

[22] K.B. Anderson, S.Y. Lockwood, R.S. Martin, D.M. Spence

A 3D-printed fluidic device that enables integrated features

Anal. Chem., 85 (2013), pp. 5622-5626

CrossRefView Record in ScopusGoogle Scholar

[23] H.N. Chan, Y.F. Chen, Y.W. Shu, Y. Chen, Q. Tian, H.K. Wu

Direct, one-step molding of 3D-printed structures for convenient fabrication of truly 3D PDMS microfluidic chips

Microfluidics and Nanofluidics, 19 (2015), pp. 9-18

CrossRefView Record in ScopusGoogle Scholar

[24] H. Gong, A.T. Woolley, G.P. Nordin

3D printed high density, reversible, chip-to-chip microfluidic interconnects

Lab on a Chip, 18 (2018), pp. 639-647

View Record in ScopusGoogle Scholar

[25] F. Li, N.P. Macdonald, R.M. Guijt, M.C. Breadmore

Using Printing Orientation for Tuning Fluidic Behavior in Microfluidic Chips Made by Fused Deposition Modeling 3D Printing

Anal. Chem. (2017)

Google Scholar

[26] M. Villegas, Z. Cetinic, A. Shakeri, T.F. Didar

Fabricating smooth PDMS microfluidic channels from low-resolution 3D printed molds using an omniphobic lubricant-infused coating

Analytica Chimica Acta, 1000 (2018), pp. 248-255

ArticleDownload PDFView Record in ScopusGoogle Scholar

[27] J. Wang, C. McMullen, P. Yao, N. Jiao, M. Kim, J.-W. Kim, L. Liu, S. Tung

3D-printed peristaltic microfluidic systems fabricated from thermoplastic elastomer

Microfluidics and Nanofluidics, 21 (2017), p. 105

CrossRefView Record in ScopusGoogle Scholar

[28] P.K. Yuen

A reconfigurable stick-n-play modular microfluidic system using magnetic interconnects

Lab on a Chip, 16 (2016), pp. 3700-3707

CrossRefView Record in ScopusGoogle Scholar

[29] C. Calderilla, F. Maya, V. Cerdà, L.O. Leal

3D-printed device for the automated preconcentration and determination of chromium (VI)

Talanta, 184 (2018), pp. 15-22

ArticleDownload PDFView Record in ScopusGoogle Scholar

[30] C.K. Su, P.J. Peng, Y.C. Sun

Fully 3D-printed preconcentrator for selective extraction of trace elements in seawater

Anal. Chem., 87 (2015), pp. 6945-6950

CrossRefView Record in ScopusGoogle Scholar

[31] V. Gupta, S. Beirne, P.N. Nesterenko, B. Paull

Investigating the effect of column geometry on separation efficiency using 3D-printed liquid chromatographic columns containing polymer monolithic phases

Anal. Chem., 90 (2017), pp. 1186-1194

View Record in ScopusGoogle Scholar

[32] V. Gupta, P. Mahbub, P.N. Nesterenko, B. Paull

A new 3D printed radial flow-cell for chemiluminescence detection: Application in ion chromatographic determination of hydrogen peroxide in urine and coffee extracts

Analytica Chimica Acta, 1005 (2018), pp. 81-92

ArticleDownload PDFView Record in ScopusGoogle Scholar

[33] E.M. Kataoka, R.C. Murer, J.M. Santos, R.M. Carvalho, M.N. Eberlin, F. Augusto, R.J. Poppi, A.L. Gobbi, L.W. Hantao, expendable Simple

3D-printed microfluidic systems for sample preparation of petroleum

Anal. Chem., 89 (2017), pp. 3460-3467

CrossRefView Record in ScopusGoogle Scholar

[34] P.J. Kitson, M.D. Symes, V. Dragone, L. Cronin

Combining 3D printing and liquid handling to produce user-friendly reactionware for chemical synthesis and purification

Chem. Sci., 4 (2013), pp. 3099-3103

View Record in ScopusGoogle Scholar

[35] L.Konieczna, M.Belka, M.Okońska, M.Pyszka, T.Bączek, New 3D-printed sorbent for extraction of steroids from human plasma preceding LC–MS analysis, *J. Chrom. A*, 15451-11.

Google Scholar

[36] P.J. Kitson, M.H. Rosnes, V. Sans, V. Dragone, L. Cronin

Configurable 3D-printed millifluidic and microfluidic ‘lab on a chip’ reactionware devices

Lab on a Chip, 12 (2012), pp. 3267-3271

CrossRefView Record in ScopusGoogle Scholar

[37] K.B. Spilstead, J.J. Learey, E.H. Doeven, G.J. Barbante, S. Mohr, N.W. Barnett, J.M. Terry, R.M. Hall, P.S. Francis

3D-printed and CNC milled flow-cells for chemiluminescence detection

Talanta, 126 (2014), pp. 110-115

ArticleDownload PDFView Record in ScopusGoogle Scholar

[38] M.D. Symes, P.J. Kitson, J. Yan, C.J. Richmond, G.J.T. Cooper, R.W. Bowman, T. Vilbrandt, L. Cronin

Integrated 3D-printed reactionware for chemical synthesis and analysis

Nat. Chem., 4 (2012), pp. 349-354

CrossRefView Record in ScopusGoogle Scholar

[39] C. Tan, M.Z.M. Nasir, A. Ambrosi, M. Pumera

3D Printed Electrodes for Detection of Nitroaromatic Explosives and Nerve Agents

Anal. Chem. (2017)

Google Scholar

[40] G. De Middleleer, P. Dubruel, S. De Saeger

Molecularly imprinted polymers immobilized on 3D printed scaffolds as novel solid phase extraction sorbent for metergoline

Analytica Chimica Acta, 986 (2017), pp. 57-70

ArticleDownload PDFView Record in ScopusGoogle Scholar

[41] U. Kalsoom, C.K. Hasan, L. Tedone, C. Desire, F. Li, M.C. Breadmore, P.N. Nesterenko, B. Paull

Low-cost passive sampling device with integrated porous membrane produced using multimaterial 3D printing

Anal. Chem., 90 (2018), pp. 12081-12089

CrossRefView Record in ScopusGoogle Scholar

[42] P. Grodzinski, J. Yang, R.H. Liu, M.D. Ward

A modular microfluidic system for cell pre-concentration and genetic sample preparation

Biomed. Microdev., 5 (2003), pp. 303-310

View Record in ScopusGoogle Scholar

[43] S.M. Langelier, E. Livak-Dahl, A.J. Manzo, B.N. Johnson, N.G. Walter, M.A. Burns

Flexible casting of modular self-aligning microfluidic assembly blocks

Lab on a Chip, 11 (2011), pp. 1679-1687

CrossRefView Record in ScopusGoogle Scholar

[44] C.E. Owens, A.J. Hart

High-precision modular microfluidics by micromilling of interlocking injection-molded blocks

Lab on a Chip, 18 (2018), pp. 890-901

View Record in ScopusGoogle Scholar

[45] M. Rhee, M.A. Burns

Microfluidic assembly blocks

Lab on a Chip, 8 (2008), pp. 1365-1373

CrossRefView Record in ScopusGoogle Scholar

[46] K.A. Shaikh, K.S. Ryu, E.D. Goluch, J.-M. Nam, J. Liu, C.S. Thaxton, T.N. Chiesl, A.E. Barron, Y. Lu, C.A. Mirkin, C. Liu

A modular microfluidic architecture for integrated biochemical analysis

Proc. Natl. Acad. Sci. U. S. A., 102 (2005), pp. 9745-9750

CrossRefView Record in ScopusGoogle Scholar

[47] P.J. Kitson, S. Glatzel, W. Chen, C.-G. Lin, Y.-F. Song, L. Cronin

3D printing of versatile reactionware for chemical synthesis

Nature Protocols, 11 (2016), p. 920

CrossRefView Record in ScopusGoogle Scholar

[48] B.C. Gross, J.L. Erkal, S.Y. Lockwood, C. Chen, D.M. Spence

Evaluation of 3D Printing and Its Potential Impact on Biotechnology and the Chemical Sciences

Anal. Chem., 86 (2014), pp. 3240-3253

CrossRefView Record in ScopusGoogle Scholar

[49] P.J. Kitson, R.J. Marshall, D. Long, R.S. Forgan, L. Cronin

3D-printed high-throughput hydrothermal reactionware for discovery, optimization, and scale-up

Angewandte Chemie Int. Edn., 53 (2014), pp. 12723-12728

CrossRefView Record in ScopusGoogle Scholar

[50] G.L. Siparsky, K.J. Voorhees, F. Miao

Hydrolysis of polylactic acid (PLA) and polycaprolactone (PCL) in aqueous acetonitrile solutions: autocatalysis

J. Environ. Polym. Degrad., 6 (1998), pp. 31-41

View Record in ScopusGoogle Scholar

[51] E.K. Sackmann, A.L. Fulton, D.J. Beebe

The present and future role of microfluidics in biomedical research

Nature, 507 (2014), p. 181

CrossRefView Record in ScopusGoogle Scholar

[52] H. Gong, B.P. Bickham, A.T. Woolley, G.P. Nordin

Custom 3D printer and resin for 18 μm \times 20 μm microfluidic flow channels

Lab on a Chip, 17 (2017), pp. 2899-2909

CrossRefView Record in ScopusGoogle Scholar

[53] H. Gong, M. Beauchamp, S. Perry, A.T. Woolley, G.P. Nordin

Optical approach to resin formulation for 3D printed microfluidics

RSC Adv., 5 (2015), pp. 106621-106632

CrossRefView Record in ScopusGoogle Scholar

[54] P.F. O'Neill, N. Kent, D. Brabazon

Mitigation and control of the overcuring effect in mask projection micro-stereolithography

AIP Conf. Proc., 1896 (2017), Article 200012

CrossRefView Record in ScopusGoogle Scholar

[55] J.C. Jokerst, J.M. Emory, C.S. Henry

Advances in microfluidics for environmental analysis

Analyst, 137 (2012), pp. 24-34

CrossRefView Record in ScopusGoogle Scholar

[56] B. Zhang, E.T. Bergström, D.M. Goodall, P. Myers

Single-particle fritting technology for capillary electrochromatography

Anal. Chem., 79 (2007), pp. 9229-9233

CrossRefView Record in ScopusGoogle Scholar

[57] G.A. Lord, D.B. Gordon, P. Myers, B.W. King

Tapers and restrictors for capillary electrochromatography and capillary electrochromatography-mass spectrometry

J. Chrom. A, 768 (1997), pp. 9-16

ArticleDownload PDFView Record in ScopusGoogle Scholar

[58] A.I. Shallan, P. Smejkal, M. Corban, R.M. Guijt, M.C. Breadmore

Cost-effective three-dimensional printing of visibly transparent microchips within minutes

Anal. Chem., 86 (2014), pp. 3124-3130

CrossRefView Record in ScopusGoogle Scholar

[59] K.C. Bhargava, B. Thompson, N. Malmstadt

Discrete elements for 3D microfluidics

Proc. Natl. Acad. Sci. U. S. A., 111 (2014), pp. 15013-15018

CrossRefView Record in ScopusGoogle Scholar

[60] E. Sisco, M. Najarro, D. Samarov, J. Lawrence

Quantifying the stability of trace explosives under different environmental conditions using electrospray ionization mass spectrometry

Talanta, 165 (2017), pp. 10-17

ArticleDownload PDFView Record in ScopusGoogle Scholar

[61] J.C. Oxley, J.L. Smith, J.E. Brady IV, A.C. Brown

Characterization and analysis of tetranitrate esters, Propellants, Explosives

Pyrotechnics, 37 (2012), pp. 24-39

CrossRefView Record in ScopusGoogle Scholar

[62] R.G. Ewing, M.J. Waltman, D.A. Atkinson, J.W. Grate, P.J. Hotchkiss

The vapor pressures of explosives

Trac-Trend Anal. Chem., 42 (2013), pp. 35-48

ArticleDownload PDFView Record in ScopusGoogle Scholar

[63] ICH

International Council for Harmonisation ICH Harmonised Tripartite Guidelines

Valid. Anal. Proced. Text Methodol. (2005)

Google Scholar

[64] R. Boopathy, J. Manning

Biodegradation of tetryl (2,4,6-trinitrophenylmethylnitramine) in a soil-slurry reactor

Water Environ. Res., 70 (1998), pp. 1049-1055

View Record in ScopusGoogle Scholar

[65] S.D. Harvey, R.J. Fellows, J.A. Campbell, D.A. Cataldo

Determination of the explosive 2,4,6-trinitrophenylmethylnitramine (tetryl) and its transformation products in soil

J. Chrom. A, 605 (1992), pp. 227-240

ArticleDownload PDFView Record in ScopusGoogle Scholar

[66] M.E. Walsh, T.F. Jenkins, S. Schnitker, J.W. Elwell, M.H. Stutz

Evaluation of SW846 Method 8330 for characterisation of sites contaminated with residues of high explosives

US Army Corps of Engineers (1993)

Google Scholar

[67] J.A. Steevens, B.M. Duke, G.R. Lotufo, T.S. Bridges

Toxicity of the explosives 2,4,6-trinitrotoluene, hexahydro-1,3,5-trinitro-1,3,5-triazine, and octahydro-1,3,5,7-tetranitro-1,3,5,7-tetrazocine in sediments to *Chironomus tentans* and *Hyalella azteca*: Low-dose hormesis and high-dose mortality

Environ. Toxicol. Chem., 21 (2002), pp. 1475-1482

View Record in ScopusGoogle Scholar

[68] S. Homma-Takeda, Y. Hiraku, Y. Ohkuma, S. Oikawa, M. Murata, K. Ogawa, T. Iwamuro, S. Li, G.F. Sun, Y. Kumagai, N. Shimojo, S. Kawanishi

2,4,6-Trinitrotoluene-induced reproductive toxicity via oxidative DNA damage by its metabolite

Free Rad. Res., 36 (2002), pp. 555-566

View Record in ScopusGoogle Scholar

[69] G.I. Sunahara, S. Dodard, M. Sarrazin, L. Paquet, G. Ampleman, S. Thiboutot, J. Hawari, A.Y. Renoux

Development of a soil extraction procedure for ecotoxicity characterization of energetic compounds

Ecotoxicol. Environ. Safe., 39 (1998), pp. 185-194

[ArticleDownload](#) [PDFView](#) [Record in Scopus](#)[Google Scholar](#)

[70] B. Lachance, P.Y. Robidoux, J. Hawari, G. Ampleman, S. Thiboutot, G.I. Sunahara

Cytotoxic and genotoxic effects of energetic compounds on bacterial and mammalian cells in vitro

Mut. Res./Genet. Toxicol. Environ. Mutagen., 444 (1999), pp. 25-39

[ArticleDownload](#) [PDFView](#) [Record in Scopus](#)[Google Scholar](#)

[71] M.E. Honeycutt, A.S. Jarvis, V.A. McFarland

Cytotoxicity and mutagenicity of 2,4,6-trinitrotoluene and its metabolites

Ecotoxicol. Environ. Safe., 35 (1996), pp. 282-287

[ArticleDownload](#) [PDFView](#) [Record in Scopus](#)[Google Scholar](#)

[72] B. Gilbert-López, F.J. Lara-Ortega, J. Robles-Molina, S. Brandt, A. Schütz, D. Moreno-González, J.F. García-Reyes, A. Molina-Díaz, J. Franzke

Detection of multiclass explosives and related compounds in soil and water by liquid chromatography-dielectric barrier discharge ionization-mass spectrometry

Anal. Bioanal. Chem., 411 (2019), pp. 4785-4796

[CrossRefView](#) [Record in Scopus](#)[Google Scholar](#)

[73] E. Holmgren, S. Ek, A. Colmsjo

Extraction of explosives from soil followed by gas chromatography-mass spectrometry analysis with negative chemical ionization

J. Chrom. A, 1222 (2012), pp. 109-115

[ArticleDownload](#) [PDFView](#) [Record in Scopus](#)[Google Scholar](#)

[74] M.E. Walsh

Determination of nitroaromatic, nitramine, and nitrate ester explosives in soil by gas chromatography and an electron capture detector

Talanta, 54 (2001), pp. 427-438